RESEARCH PAPER

Cancer Biology & Therapy 15:7, 862–877; July 2014; © 2014 Landes Bioscience

Inhibition of Notch signaling alters the phenotype of orthotopic tumors formed from glioblastoma multiforme neurosphere cells but does not hamper intracranial tumor growth regardless of endogene Notch pathway signature

Karina Kristoffersen[1,*], Mette Kjølhede Nedergaard[2], Mette Villingshøj[1], Rehannah Borup[3], Helle Broholm[4], Andreas Kjær[2], Hans Skovgaard Poulsen[1], and Marie-Thérése Stockhausen[1]

[1]Department of Radiation Biology; The Finsen Center; Copenhagen University Hospital; Copenhagen, Denmark; [2]Department of Clinical Physiology, Nuclear Medicine & PET and Cluster for Molecular Imaging; Copenhagen University Hospital and University of Copenhagen; Copenhagen, Denmark; [3]Center for Genomic Medicine; Copenhagen University Hospital; Copenhagen, Denmark; [4]Department of Neuropathology; The Diagnostic Center; Copenhagen University Hospital; Copenhagen, Denmark

Keywords: glioblastoma multiforme, neurosphere culture, orthotopic xenograft, brain cancer stem-like cells, Notch signaling, Notch activity, DAPT

Abbreviations: bCSC, brain cancer stem-like cells; DAPT, N-[N-(3,5-difluorophenacetyl-L-alanyl)]-S-phenylglycine *t*-butyl ester; GBM, glioblastoma multiforme; GSI, γ-secretase inhibitor; NSC, neural stem cells

Background: Brain cancer stem-like cells (bCSC) are cancer cells with neural stem cell (NSC)-like properties found in the devastating brain tumor glioblastoma multiforme (GBM). bCSC are proposed a central role in tumor initiation, progression, treatment resistance and relapse and as such present a promising target in GBM research. The Notch signaling pathway is often deregulated in GBM and we have previously characterized GBM-derived bCSC cultures based on their expression of the Notch-1 receptor and found that it could be used as predictive marker for the effect of Notch inhibition. The aim of the present project was therefore to further elucidate the significance of Notch pathway activity for the tumorigenic properties of GBM-derived bCSC.

Methods: Human-derived GBM xenograft cells previously established as NSC-like neurosphere cultures were used. Notch inhibition was accomplished by exposing the cells to the gamma-secretase inhibitor DAPT prior to gene expression analysis and intracranial injection into immunocompromised mice.

Results: By analyzing the expression of several Notch pathway components, we found that the cultures indeed displayed different Notch pathway signatures. However, when DAPT-treated neurosphere cells were injected into the brain of immunocompromised mice, no increase in survival was obtained regardless of Notch pathway signature and Notch inhibition. We did however observe a decrease in the expression of the stem cell marker Nestin, an increase in the proliferative marker Ki-67 and an increased number of abnormal vessels in tumors formed from DAPT-treated, high Notch-1 expressing cultures, when compared with the control.

Conclusion: Based on the presented results we propose that Notch inhibition partly induces differentiation of bCSC, and selects for a cell type that more strongly induces angiogenesis if the treatment is not sustained. However, this more differentiated cell type might prove to be more sensitive to conventional therapies.

Introduction

The brain tumor glioblastoma multiforme (GBM) is among the most lethal malignancies in adults and it affects 3.5/100 000 persons every year in western countries.[1] The survival probability is 57% the first year after diagnosis and recurrence is reported in 99% of patients within seven years,[2] which is why GBM is thus far considered incurable. Brain cancer stem-like cells (bCSC) present a novel target in the search for improved anti-GBM therapy as they are suggested to play a pivotal role in tumor initiation, progression, treatment resistance and relapse.[3-8] The bCSC are characterized by their neural stem cell (NSC)-like features and tumorigenic properties, as they possess self-renewing and multipotent abilities as well as in vivo tumor forming potential.[3,9-11] The search for regulators that might be of importance for maintaining the bCSC population is thus considered a key quest in

*Correspondence to: Karina Kristoffersen; Email: karina.kristoffersen@mail.com
Submitted: 02/08/2014; Revised: 03/24/2014; Accepted: 04/13/2014; Published Online: 04/22/2014
http://dx.doi.org/10.4161/cbt.28876

GBM research. The Notch signaling pathway is known to be important for maintenance of the normal NSC population during development as this pathway regulates the balance between the NSC pool and its differentiated progeny.[12,13] It is believed that the outcome of Notch signaling in cancer reflects its role in the development of the corresponding normal tissue. In this context it has been demonstrated that Notch signaling often is deregulated in GBM[14-16] and that bCSC are sensitive to Notch inhibition.[16-18] Elevated expression of Notch signaling pathway components has recently been associated with the classical GBM sub-type identified by global gene expression.[19] Sub-grouping of GBM tumors based on gene expression could potentially assist clinicians in the future when stratifying patients to the most optimal targeted treatment as has been the case for receptor tyrosine kinase HER2 and estrogen receptor positive breast cancers.[20-22] Thus, by classifying GBM tumors into different sub-types it might be possible to identify new molecular targets, essential for maintenance of a specific sub-type. In line with this, we have previously shown that the level of Notch activity is predictive for the effect of Notch inhibition in GBM neurosphere cultures in vitro, as growth and stem cell-like features only were affected in cultures with high Notch expression and activity.[23]

In the present study, we sought to further classify the GBM neurosphere cultures previously used[23,24] by global gene expression analysis and assign them a possible Notch signature. In addition, the cultures were established as intracranial tumors in order to further determine the relevance of active Notch signaling for tumor formation. We found that neurosphere cultures with high endogenous Notch-1 expression, and elevated expression of a Notch pathway signature, formed tumors with a more infiltrative phenotype than neurosphere cultures with low Notch-1 expression, and Notch pathway signature. However, in contrast to what was expected, we did not observe increased survival when we injected cells pretreated with the Notch inhibitor DAPT as compared with a control treatment. We did, nevertheless, find that some of the tumors formed from DAPT treated cultures displayed lower levels of the stem cell marker Nestin and increased number of proliferative cells as well as abnormal vessels. In addition, the global gene expression analysis suggested that DAPT treatment increased both the angiogenic potential and the differentiation level of the cells. Based on our findings we suggest, despite indications of increased aggressiveness, that bCSC targeted anti-Notch treatment in combination with traditional therapy might be feasible, as Notch inhibition possibly induces the bCSC population to differentiate which could imply increased sensitivity to chemo- and radiation therapy.

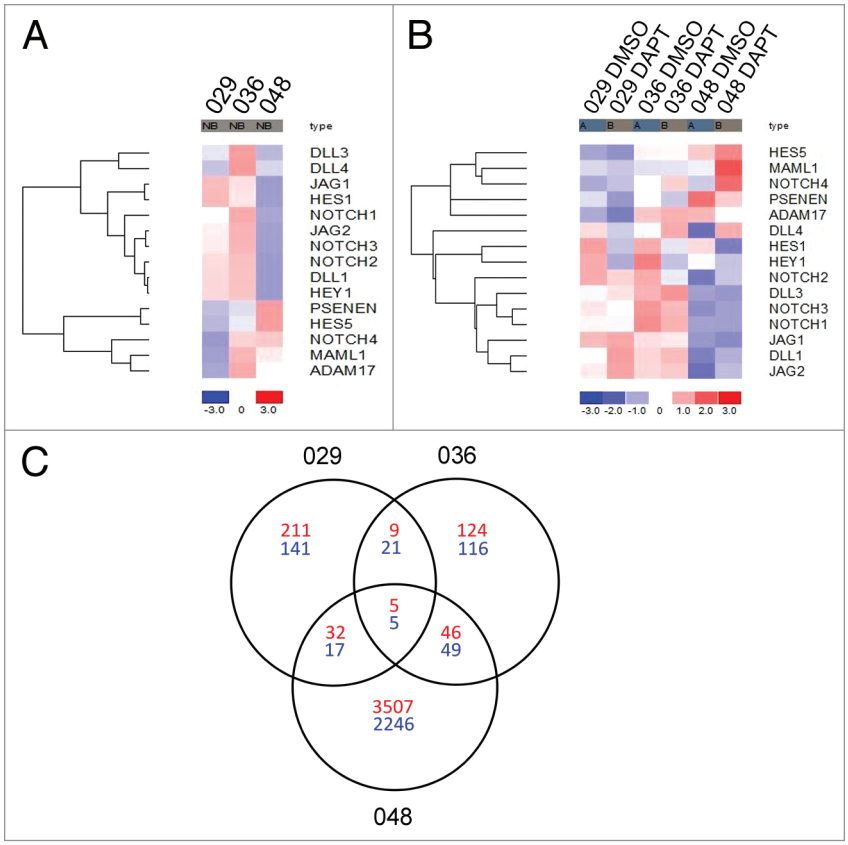

Figure 1. Gene expression analysis revealed different Notch signatures between the GBM neurosphere cultures investigated. (**A**) Heat map showing the expression of selected Notch pathway components in the 029, 036, and 048 neurosphere cultures. (**B**) Heat map showing the expression of the same components in the same neurosphere cultures treated with 10 μM DAPT or equal volumes of DMSO for 24 h. In both (**A and B**) the colors represent the standard deviation in expression level relative to the mean expression of the respective gene across the three or six samples respectively. (**C**) Venn diagram showing the intersection of the differently expressed genes for each culture with a fold change of minimum ± 1.3. Red numbers refer to upregulated genes in the DAPT treated samples compared with the DMSO control and blue numbers refer to downregulated genes.

Results

Microarray analysis and Notch signature

We have previously categorized the 029 and 036 neurosphere cultures as having high endogenous Notch-1 expression and Notch pathway activation, as indicated by high Hes-1 expression, when compared with the 048 culture which we have classified as having low Notch-1 expression and activation. We have also shown that Notch inhibition by DAPT treatment did not affect the 048 culture to the same degree as the 029 and 036 cultures.[23] To elaborate this, we performed a global gene expression analysis and used this to establish a possible Notch signature of the three cultures. The expression of selected Notch pathway components is shown in **Figure 1A**. (For the expression of all Notch pathway components included in the "KEGG_Notch_signaling_pathway" gene set, see **Fig. S1**). As displayed in **Figure 1A**, the 048 culture differed from the 029 and 036 cultures, with regard to the majority of the Notch components shown. Notably, the Notch-1, -2, and -3 receptors, the ligands Delta-like (DLL) -1,

Jagged-1 and -2, and the downstream targets Hes-1 and Hey-1 were all expressed at a lower level in 048 compared with 029 and 036, indicating a higher activity of the Notch pathway in the two latter cultures. Conversely, the transcriptional target Hes-5 was expressed at a higher level in 048 as compared with 029 and 036 and the Notch-4 receptor was expressed at the lowest level in 029. Moreover, the ligands Dll-3 and -4 showed a higher expression level in the 036 culture as compared with the 029 and 048 cultures. We next analyzed the expression of the same genes in cultures treated with 10 μM DAPT or equal volumes of DMSO for 24 h. As seen in **Figure 1B**, Hes-1 and Hey-1 were downregulated upon DAPT treatment in all three cultures verifying successful Notch inhibition and showing that some degree of Notch signaling was present also in the 048 culture. Furthermore, the γ-secretase sub-unit PSENEN was downregulated in all cultures, while DLL-1 was upregulated, a tendency also shown for Notch-4, DLL-3, and Jagged-2.

In order to examine to what extent the effect of DAPT treatment showed overlap between the cultures we visualized the intersection of differentially expressed transcripts (minimum fold change ± 1.3) between DMSO and DAPT treatment in the three cultures in a Venn diagram. In **Figure 1C**, the number of transcripts that were upregulated in the DAPT treated cultures compared with the control is presented in red and the number of downregulated transcripts in blue. Only annotated transcripts (probe sets that have been assigned a gene symbol) are presented. The gene symbol and title of the annotated transcripts that were up- or downregulated between the 029 and 036 cultures and between all three cultures is displayed in **Table 1**. In summary, five transcripts were consistently downregulated and five transcripts were upregulated in all three cultures (**Fig. 1C**). The transcriptional Notch targets Hes-1 and Hey-1 were both represented among the transcripts consistently downregulated in all three cultures, verifying successful inhibition of Notch signaling, together with the ephrin-B2 (EFNB2), eyes shut homolog (EYS), and the GABA-B2 receptor (GABBR2) (**Table 1**). In addition, nine upregulated and 21 downregulated transcripts were in common between the 029 and 036 cultures (**Fig. 1C**), although the majority of up- and downregulated transcripts were differentially regulated in these cultures. Finally, the amount of transcripts either up or downregulated was much higher in the 048 culture compared with the 029 and 036 cultures (**Fig. 1C**).

Different neurosphere cultures give rise to intracranial tumors with different features, but all display GBM characteristics

To extend our in vitro findings, that the different neurosphere cultures displayed different characteristics such as growth- and gene expression patterns (as presented above and in ref. 23) we engrafted the neurosphere cells in vivo in order to examine whether the cultures also formed dissimilar tumors. When injected into the brains of immunocompromised mice, all neurosphere cultures formed intracranial tumors verifying their tumorigenic potential. However, there was a considerable difference in the time from injection to when the mouse had to be euthanized, between the cultures. In **Figure 2A**, the survival in weeks of mice injected with control treated 029, 036, or 048 cells is presented. Mice injected with 036 cells survived the longest namely 29.60 wk (95% CI: 20.88–38.32), while mice injected with 029 neurosphere cells survived approximately 17.20 wk (95% CI: 15.58–18.82) and mice injected with 048 cells had the shortest survival at 6.25 wk (95% CI: 4.73–7.77). Furthermore, mice injected with 036 cells showed the highest variability in survival, from 19 to 38 wk, while the survival of mice injected with 048 cells varied from 5 to 7 wk. The histological appearance of the tumors also varied greatly, especially when comparing the 029 and 036 tumors with the 048 tumors. Representative H&E sections of tumors formed from control treated neurosphere cultures are displayed in **Figure 2B**. In general, the 048 tumors were mostly uniform in appearance with a well-defined border between the tumor and the surrounding normal brain parenchyma, whereas the 029 and 036 tumors were much more disorganized with no clear border and especially the 036 tumors tended to home to the ventricles (for additional H&E pictures, see **Fig. S2**). Using ^{18}F-FET PET/CT scanning we were furthermore able to detect in situ tumor formation in mice injected with cells from each of the three cultures and it was as such possible to follow tumor growth in real-time. In **Figure 2C**, coronal views of the ^{18}F-FET PET/CT scannings of one representative mouse at week 1, 4, 5, and 6 after injection with 048 neurosphere cells are presented. The mouse was euthanized at week 7. However, it was not possible to include the mice used for ^{18}F-FET PET/CT scans in the survival data, as they did not tolerate the weekly sedation well and had to be euthanized due to symptoms not certainly related to tumor formation. Histological GBM hallmarks were evident in tumors from all neurosphere cultures used and representative H&E stainings showing mitosis, invasion, necrotic areas with pseudopalisading cells, and excessive vascularization are presented in **Figure 2D**. It should be noticed that the vessels did not exhibit an abnormal/malignant phenotype in the tumors formed from control treated cells. Finally, by evaluating the expression of the Notch-1 receptor in the intracranial tumors using IHC staining, we found that the 048 tumors tended to display a weaker staining intensity as compared with the 029 and 036 tumors indicating a lower expression of Notch-1 in these tumors, which is in good correlation with our in vitro observations. Representative pictures are displayed in **Figure 2E**.

Notch inhibition in neurosphere cells does not hamper intracranial tumor formation and growth

We have previously demonstrated that pre-treating the 029 and 036 cells with DAPT almost abolished their ability to form clonogenic colonies in soft agar possibly as a consequence of slowing of the cell cycle, whereas no effect was seen on the 048 cells.[23] To determine if inhibition of Notch signaling prior to xenoengraftment also affected the ability of intracranial tumor growth, we treated the 029, 036, and 048 neurosphere cells with 10 μM DAPT ex vivo for seven days and then injected 100 000 viable cells stereotactically into the brains of C.B-17 SCID mice. DMSO was used as a control treatment. Each individual mouse was monitored frequently during the experiment and was euthanized when it showed tumor related symptoms and/or considerable weight loss (**Fig. S3**).

Table 1. Annotated transcripts consistently regulated between the cultures

Upregulated in DAPT vs. DMSO	
029, 036	MIR186: microRNA186
	LINC00341: long intergenic non-protein coding RNA 341
	TRNAL46P: tRNA leucine 46 (anticodon UAA) pseudogene
	DSG2: desmoglein 2
	HCAR2: hydroxycarboxylic acid receptor 2
	ZNF578: zinc finger protein 578
	SEPP1: selenoprotein P, plasma, 1
	LOC100506127: putative uncharacterized protein FLJ37770-like
	HSD17B7P2: hydroxysteroid (17-β) dehydrogenase 7 pseudogene 2
029, 036, 048	CEACAM5: carcinoembryonic antigen-related cell adhesion molecule 5, *P = 0.17*
	RN5S341: RNA, 5S ribosomal 341, *P = 0.24*
	RN5S331: RNA, 5S ribosomal 331, *P = 0.015*
	RNY3P3: RNA, Ro-associated Y3 pseudogene 3, *P = 0.48*
	EPCAM: epithelial cell adhesion molecule, *P = 0.0068*
Downregulated in DAPT vs. DMSO	
029, 036	RPE65: retinal pigment epithelium-specific protein 65kDa
	RNU6–14: RNA, U6 small nuclear 14
	SNORD115–41: small nucleolar RNA, C/D box 115–41
	TUBB8: tubulin, β 8 class VIII
	RN5S121: RNA, 5S ribosomal 121
	CDRT1 /// FBXW10: CMT1A duplicated region transcript 1 /// F-box and WD repeat domain containing 10
	RN5S374: RNA, 5S ribosomal 374
	RNY4P5: RNA, Ro-associated Y4 pseudogene 5
	KAL1: Kallmann syndrome 1 sequence
	VGF: VGF nerve growth factor inducible
	PTK2B: PTK2B protein tyrosine kinase 2 β
	HBEGF: heparin-binding EGF-like growth factor
	SCG2: secretogranin II
	GPX3: glutathione peroxidase 3 (plasma)
	FBLN5: fibulin 5
	CFHR4: complement factor H-related 4
	HHIP: hedgehog interacting protein
	GPC1: glypican 1
	TTYH1: tweety homolog 1 (*Drosophila*)
	CHL1: cell adhesion molecule with homology to L1CAM (close homolog of L1)
	PDE10A: phosphodiesterase 10A
029, 036, 048	EFNB2: ephrin-B2, *P = 0.082*
	EYS: eyes shut homolog, *P = 0.010*
	HES1: hairy and enhancer of split 1, *P = 0.0080*
	HEY1: hairy/enhancer-of-split related with YRPW motif 1, *P = 0.079*
	GABBR2: gamma-aminobutyric acid (GABA) B receptor, 2, *P = 0.067*

Transcripts consistently regulated between the 029 and 036 cultures and between the 029, 036, and 048 cultures are shown in the table by their gene symbol and title. *P* value represents paired *t* test between control and treated groups with $n = 3$, why no *P* value is presented for the annotated transcripts regulated between the 029 and 036 cultures.

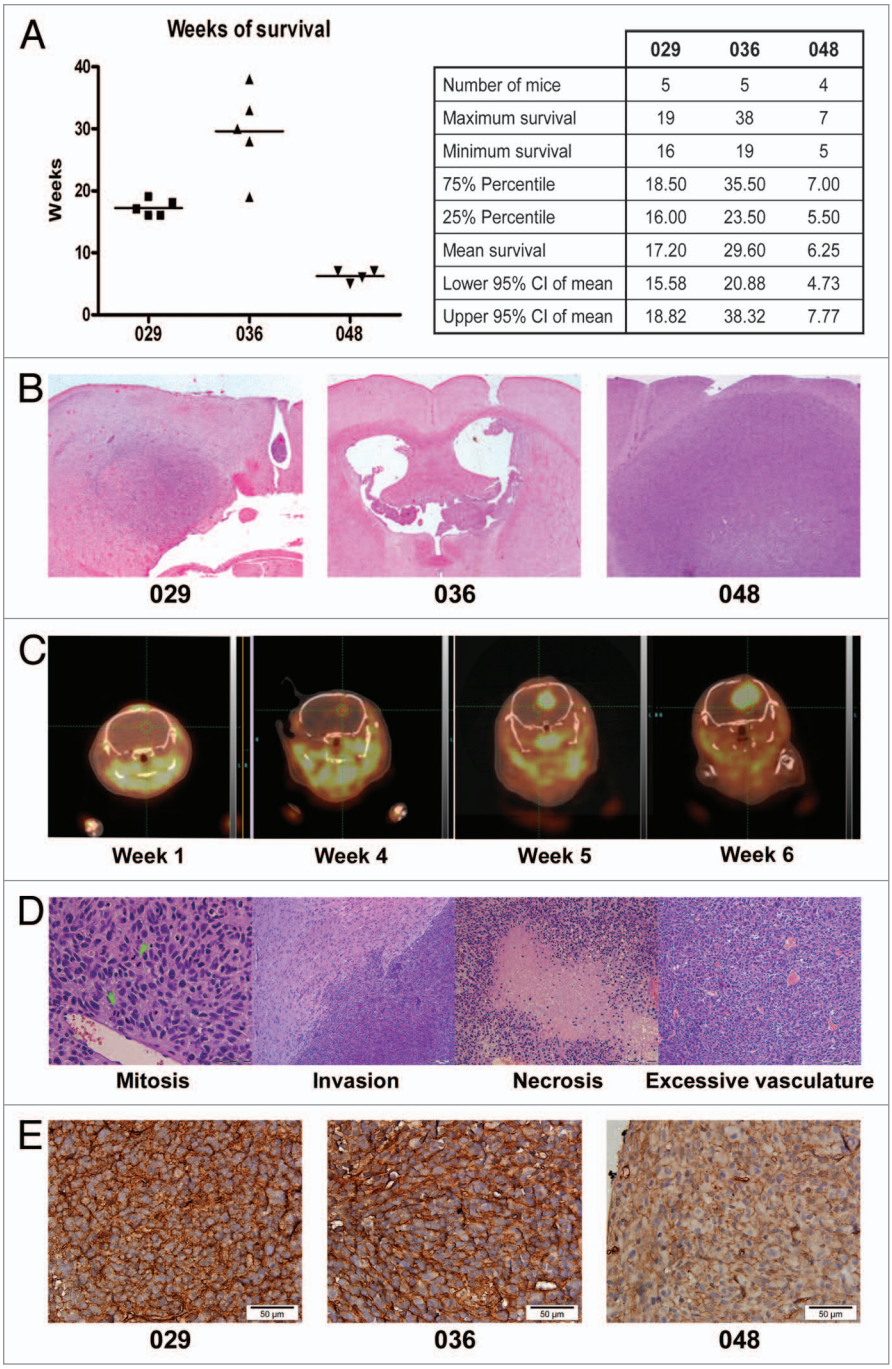

	029	036	048
Number of mice	5	5	4
Maximum survival	19	38	7
Minimum survival	16	19	5
75% Percentile	18.50	35.50	7.00
25% Percentile	16.00	23.50	5.50
Mean survival	17.20	29.60	6.25
Lower 95% CI of mean	15.58	20.88	4.73
Upper 95% CI of mean	18.82	38.32	7.77

Figure 2. GBM cells from different neurosphere cultures form tumors with different phenotypes when injected into mouse brains. (**A**) Survival in weeks of mice injected with 029, 036, or 048 neurosphere cells treated with the control substance DMSO for 1 wk prior to injection. Dot plot and column statistics were generated using the GraphPad Prism 4 software (GraphPad Software, http://www.graphpad.com). (**B**) Representative H&E staining of the tumors displayed in (**A**). (**C**) ^{18}F-FET PET/CT scans of a mouse injected with DMSO-treated 048 cells at week 1, 4, 5, and 6 after injection. (**D**) Representative H&E pictures of the intracranial tumors showing characteristics of high grade gliomas i.e., mitosis and invasion and GBM specific hallmarks i.e., necrosis and excessive vasculature. Green arrows indicate mitotic cells. (**E**) Representative immunohistochemical stainings of the Notch-1 receptor in tumors formed from 029, 036, and 048 control treated neurosphere cells, respectively. Scale bar shows 50 µm.

To test if Notch signaling was inhibited in the injected cells at the time of intracranial injection, the Notch-1 protein level and the activity of the Notch pathway, as assessed by Hes-1 expression were analyzed in DAPT and control treated samples generated in parallel to the cells injected. As expected, Notch-1 and Hes-1 were expressed at higher levels in the control treated 029 and 036 cultures as compared with the 048 culture (**Fig. 3A**), which verifies our previous findings.[23] Furthermore, a prominent downregulation of Hes-1, indicative for Notch pathway inhibition, could be detected in 029 and 036 DAPT treated samples when compared with the control, whereas the downregulation was not as evident in the 048 culture. We thus concluded that Notch signaling was inhibited in the DAPT treated cells that were intracranially injected. However, as displayed in **Figure 3B and D**, there was no statistical difference in survival between mice injected with DAPT-treated 029 cells (P = 0.32) or DAPT-treated 048 cells (P = 0.22) when compared with DMSO-treated cells, indicating that there was no major difference in intracranial tumor growth between the control and DAPT-treated groups. There was, however surprisingly, a small decrease in survival for mice injected with DAPT-treated 036 cells when compared with DMSO-treated 036 cells (P = 0.037) (**Fig. 3C**).

Tumors formed from DAPT-treated cultures show increased differentiation and angiogenesis

In order to assess histology of the intracranial tumors, we stained histological sections from three different intracranial tumors for each of the three tumor-types in each treatment group (representative pictures are shown in **Fig. 4** and additional H&E pictures are shown in **Fig. S2**). As visualized by H&E staining, DAPT treated 036 cells tended to form highly vascularized tumors with large voluminous vessels (**Fig. 4D**). Three out of three 036 DAPT tumors evaluated demonstrated this phenotype which was also observed in one out of three 029 DAPT tumors (**Fig. S2**). No obvious difference was observed between 048 DMSO and DAPT tumors (**Fig. 4E and F**). The stem cell marker Nestin, was evaluated by staining intensity, distinguishing between if all tumor cells were highly positive and if they in general displayed a more pale coloration,

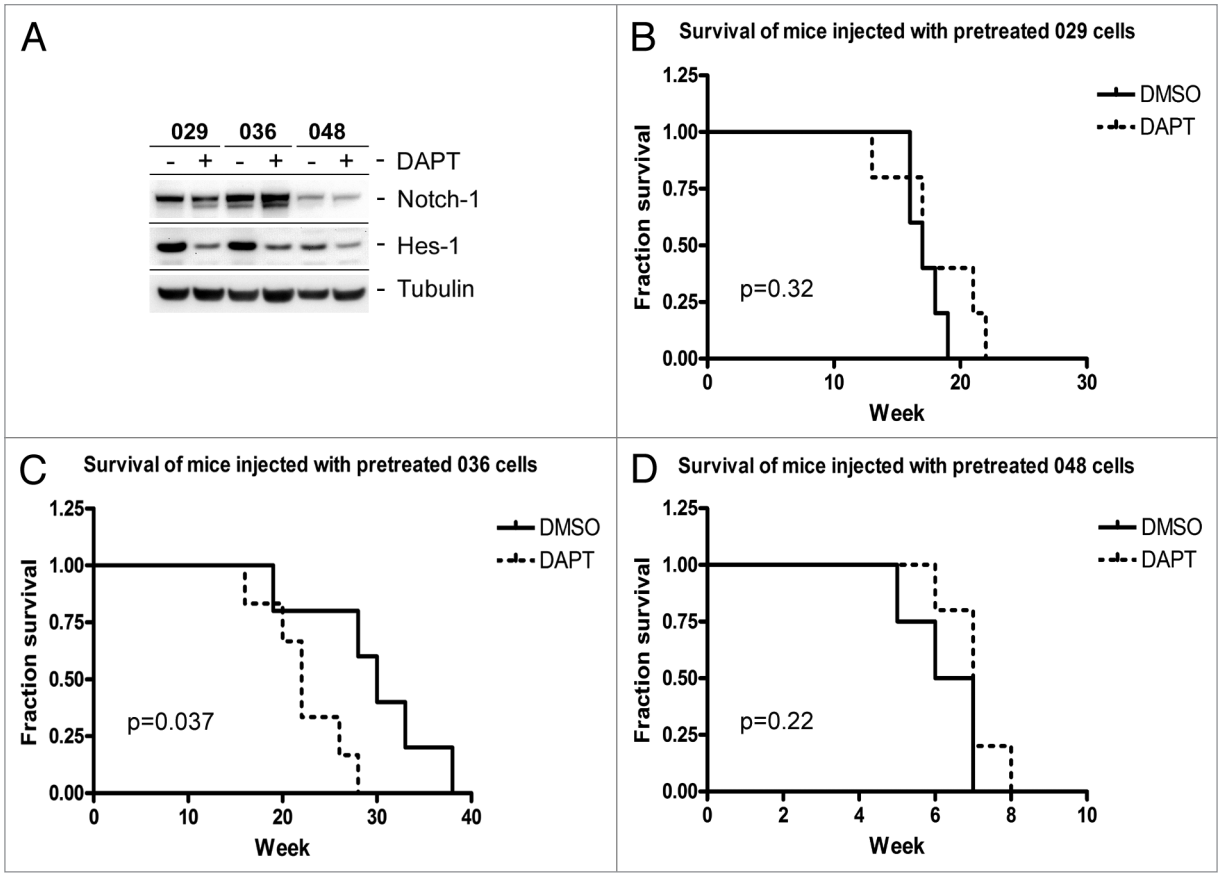

Figure 3. No survival benefit for mice injected with DAPT treated GBM neurosphere cells. (**A**) WB showing expression of the Notch-1 receptor and the Notch transcriptional target Hes-1 in GBM neurosphere cells treated with DMSO for control (–) or 10 μM DAPT (+) for seven days, prior to intracranial injection. (**B–D**) Kaplan-Meyer plots showing the fractionated survival of mice injected with (**B**) 029, (**C**) 036, or (**D**) 048 cells pretreated for one week with either 10 μM DAPT or equal volumes of DMSO. *P* values represent the comparison of survival curves by log-rank test performed in the GraphPad Prism 4 software.

or if there existed areas within the tumor tissue that were negative (marked "+" and "(+)" respectively in **Table 2**). We found that all DMSO tumors, regardless of origin showed high expression of Nestin in all tumor cells (**Table 2**; **Fig. 4G, I, and K**). The same was the case for all 048 DAPT tumors (**Table 2**; **Fig. 4L**). In contrast three out of three 029 DAPT tumors and one out of three 036 DAPT tumors showed a decreased expression of Nestin (**Table 2**), either by displaying a general weaker staining in the tumor cells (exemplified by 029 in **Fig. 4H**) or by containing areas with almost no Nestin positive cells (exemplified by 036 in **Fig. 4J**). The proliferation marker Ki-67 was analyzed by evaluating the fraction of Ki-67 positive nuclei. In **Table 2** less than 25% positive nuclei is annotated "+" and more that 25% is annotated "++". As such, we found no difference in the fraction of proliferative cells between 029 DMSO and DAPT tumors or in 048 DMSO and DAPT tumors (**Table 2**; **Fig. 4M, N, Q, and R**). In contrast the 036 DMSO tumors displayed the lowest fraction of proliferative cells which was increased in the 036 DAPT tumors (**Table 2**; **Fig. 4O and P**). Finally, the endothelial cell marker CD31 was assessed by the presence of abnormal vessels. No abnormal vessels in the section was assigned "–", few abnormal vessels (1–10) was assigned "(+)", and high density of abnormal vessels was assigned "+". None of the DMSO tumors displayed any abnormal vessels (**Table 2**; **Fig. 4S, U, and X**). However, abnormal vessels were observed in one out of three of the 029 DAPT tumors and three out of three 036 DAPT tumors (**Table 2**; **Fig. 4T and V**). Furthermore, two out of three 048 DAPT tumors showed a few small abnormal vessels (**Fig. 4Y**). As the antibody we initially used to stain endothelial cells detected both murine and human CD31, we subsequently included a human specific CD31 antibody in order to analyze the origin of the intra-tumoral vessels. However, none of the tumors were positive for this marker, when compared with positive control tissue (**Fig. 5**).

The angiogenic and stem cell-like expression profile is differentially altered upon Notch inhibition

As the IHC analyses indicated that the angiogenic and stem cell-like phenotype was altered in some of the DAPT tumors compared with the control, we extracted selected pro-angiogenic markers as well as markers for NSC and differentiation from the global gene expression data and performed hierarchical cluster analyses. The selected pro-angiogenic markers in **Figure 6A** were in general differently regulated upon DAPT treatment in the three cultures when compared with the DMSO control, although a few correlations could be noticed. As such,

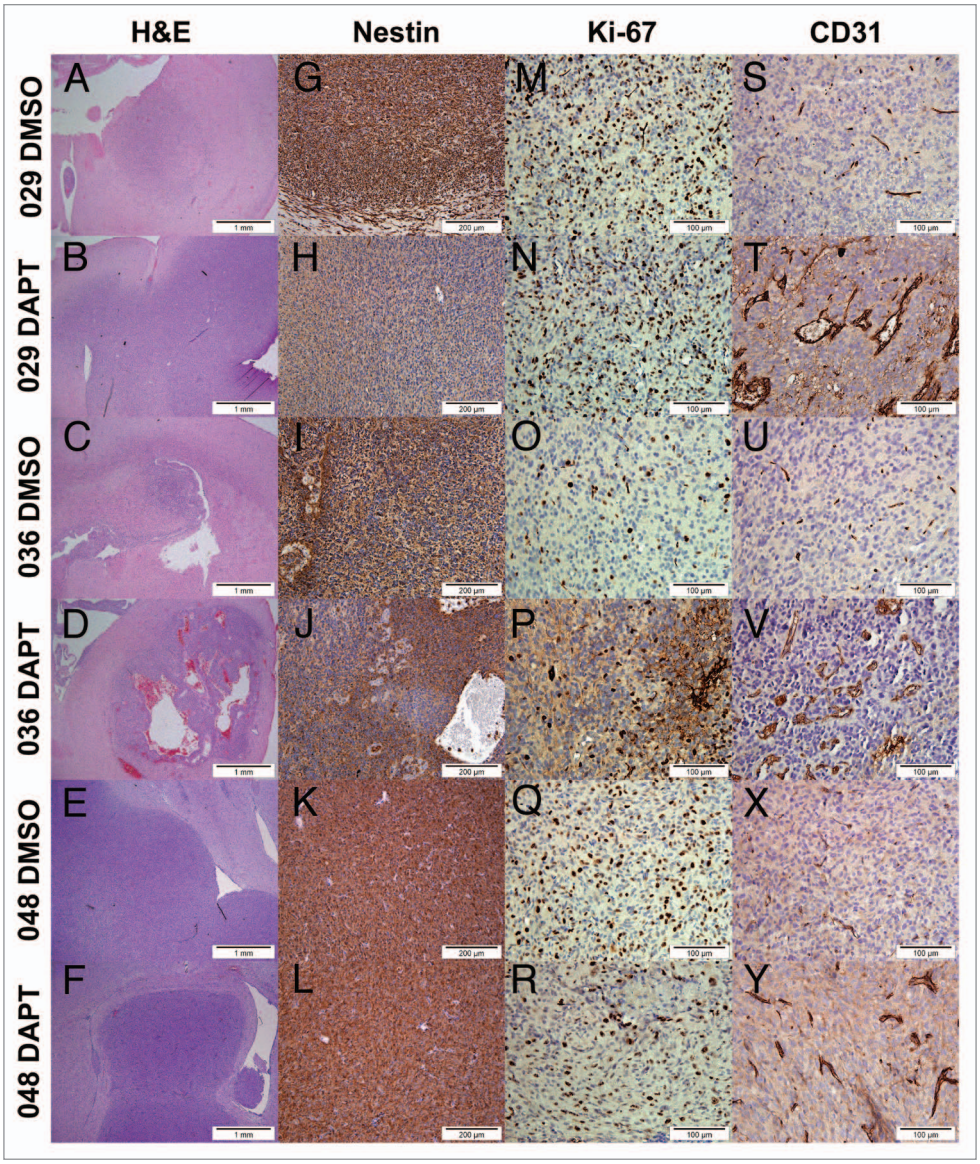

Figure 4. Histology and expression of the stem cell marker Nestin, the proliferative marker Ki-67 and the endothelial cell marker CD31 differed between tumors formed from DMSO and DAPT-treated neurosphere cells. (**A–F**) H&E of representative tumors from each treatment group of the three tumor-types. Scale bar shows 1 mm. (**G–L**) Immunodetection of the stem cell marker Nestin. Positive cells stain dark brown in the cytoplasm. Scale bar shows 200 μM. (**M–R**) Immunodetection of the proliferative marker Ki-67. Positive nuclei are stained dark brown. Scale bar shows 100 μM. (**S–Y**) Immunodetection of the endothelial marker CD31. Normal vessels are shown as strait brown stripes in the section, while abnormal vessels are detected as disorganized vessels often with multiple endothelial cells constituting the vessel wall. Scale bar shows 100 μM.

the cadherin CDH13, the stabilin STAB1 and the interleukin IL18 were upregulated in all three cultures whereas the vascular endothelial growth factor VEGFA and the platelet-derived growth factor PDGFA only were upregulated in 029 and 036, but not in 048. In **Figure 6B**, expression of selected NSC markers and markers of the three neural lineages (notice that some markers represent more than one phenotype, e.g., GFAP is a marker for both NSC and astrocytes) is displayed. Of the NSC markers (PROM1, NES, NOTCH1, NOTCH2, GFAP, CXCR4, SOX1, SOX4, PDGFRA, RXRA, and VIM), Nestin (NES) was the only marker downregulated in all three cultures upon DAPT treatment, while SOX4 was slightly upregulated in all three cultures. Of the neuronal markers (TUBB3, NEFM, MAP2, and DCX), neurofilament (NEFM) was upregulated in all cultures, βIII-tubulin (TUBB3) was upregulated in 029 and 036, and Doublecortin (DCX) was upregulated in 036 and 048 while downregulated in 029. Finally, of the glial markers (GFAP, GALC, CNP, PDGFRA, VIM, OLIG1, and OLIG2), the oligodendrocyte transcription factor 1 (OLIG1) was upregulated in all three cultures, although most prominent in 029 and 048, GALC was downregulated in 036 and GALC, together with GFAP, was slightly upregulated in 048. A simplified overview of the regulation of the NSC and differentiation markers outlined above is given in **Table 3**.

Discussion

In the latter years researchers have attempted to sub-type GBM based on global gene expression and proteomics.[19,25,26] In the future this sub-typing is thought to assist clinicians in stratifying GBM patients to the most optimal therapy as has proven possible with MGMT methylation and temozolomide (TMZ, Temodal®) treatment.[27] As such, it is believed that the different sub-types display molecular hallmarks that are of specific importance for each sub-type. Accordingly, the Notch signaling pathway has been associated with the classical sub-type.[19] We have previously shown that the 029 and 036 patient-derived xenograft tumors and thereof derived neurosphere cultures could be characterized as having high Notch-1 and Hes-1 expression while 048 xenograft tumors and cultures were characterized as having low Notch-1 and Hes-1 expression,[23] indicating that they belong to different GBM sub-types. It should, however, be held in mind that sub-typing of in vitro cultures is not yet confirmed comparable with patient tumor sub-types.[19] In the present study we have sought to elaborate our previous findings, by analyzing the global gene expression pattern of the three cultures and further study the effect of Notch inhibition on intracranial tumor growth. Overall, we found that the three cultures examined in the present project display different activation of the Notch signaling pathway, with the 029 and 036 most likely representing cultures with an elevated Notch signaling signature as compared with the 048 culture. However, there was no survival benefit for mice injected with Notch inhibited neurosphere cells regardless of the Notch signature.

Although the specific 029 and the 036 cultures used in the present study showed the highest degree of similarity with regard to expression of Notch pathway components, and most likely are originated from the same patient tumor as described in the materials and methods section, GBM neurosphere cultures paragraph, they are not alike. This is evident as the 036 culture expressed the highest level of the ligands DLL3 and DLL4 whereas the expression in 029 was similar to the one in 048. Dll expression is seen in proneuronal cells[28] which could indicate that the 036 culture was established from a xenograft tumor with a more neuronal phenotype than the xenograft tumors from where the 029 and 048 tumors were derived. This also suggests that the respective xenograft tumors from where the 029 and 036 cultures were established might represent different clones of the same original tumor that nevertheless both showed high Notch pathway activity. Moreover, 029 showed the lowest level of the Notch-4 receptor, the metalloprotease ADAM17 and the downstream effector MAML1 while expression of these components in 036 was similar to 048. The difference between the 029 and 036 cultures is further supported when evaluating the growth pattern both in vitro and in vivo as well as the effect from Notch inhibition (in this and our previous study[23]). As an example only 40 out of 776 transcripts were similarly regulated between the 029 and 036 cultures upon DAPT treatment as visualized in the Venn diagram. This supports our notion that, although STR-profiling suggests that the specific 029 culture used (GBM_CPH029p7, established from a mouse xenograft passage 7[23,24]) most likely originates from the GBM_CPH036 patient tumor, it has developed as an individual culture over the years. For this and the previous study[23] we have therefore chosen to treat the GBM_CPH029p7 and the NGBM_CPH036p7 cultures as two individual GBM neurosphere cultures with an elevated Notch pathway signature, based on the high expression level of Notch-1, -2, and -3 receptors, the ligands DLL-1, Jagged-1, and -2, and the downstream targets Hes-1 and Hey-1, compared with the 048 culture. Moreover, the conclusion of this and the previous study[23] remains unchanged as they both are based on the difference in effect of Notch inhibition on cultures with different Notch pathway activation.

When looking at the overall change in gene expression upon DAPT treatment between the three cultures it becomes clear that far more transcripts were affected by DAPT treatment in 048, than in 029 and 036. The high level of Notch-4 and Hes-5 in 048 further indicates that the Notch signaling pathway, at least to some degree, is active also in the 048 culture. However, as this culture seems to be less sensitive to DAPT treatment on a functional level, the transcripts affected in the 048 culture might not be as relevant with regard to NSC-like and growth potential.[23] An active Notch signaling in 048 is further supported by downregulation of the Notch pathway transcriptional targets Hes-1 and Hey-1 in this culture as well. On the contrary Hes-5 seems to be

Table 2. IHC evaluation of intracranial tumors formed from DAPT- and DMSO-treated GBM neurosphere cultures

Cells injected	Pretreated with	Nestin	Ki-67	CD31
029	DMSO	+	++	–
		+	N.A.	–
		+	++	–
	DAPT	(+)	++	–
		(+)	++	–
		(+)	++	+
036	DMSO	+	+	–
		+	+	–
		+	+	–
	DAPT	(+)	++	+
		+	++	+
		+	++	+
048	DMSO	+	++	-
		+	N.A.	N.A.
		+	++	–
	DAPT	+	++	–
		+	++	(+)
		+	++	(+)

Nestin, CD31 and Ki-67 expression in brain sections from mice injected intracranial with DAPT or DMSO treated neurosphere cells. **Nestin**: "+" = all tumors cells were highly positive for Nestin, "(+)" = either a more pail coloration of the tumor tissue in general or areas within the tumor tissue that are negative for Nestin. **Ki-67**: "+" = less than 25% positive nuclei and "++" = more than 25% positive nuclei. **CD31**: "–" = no abnormal vessels, "(+)" = between 1 and 10 abnormal vessel in the section and "+" more than 10 abnormal vessels in the section.

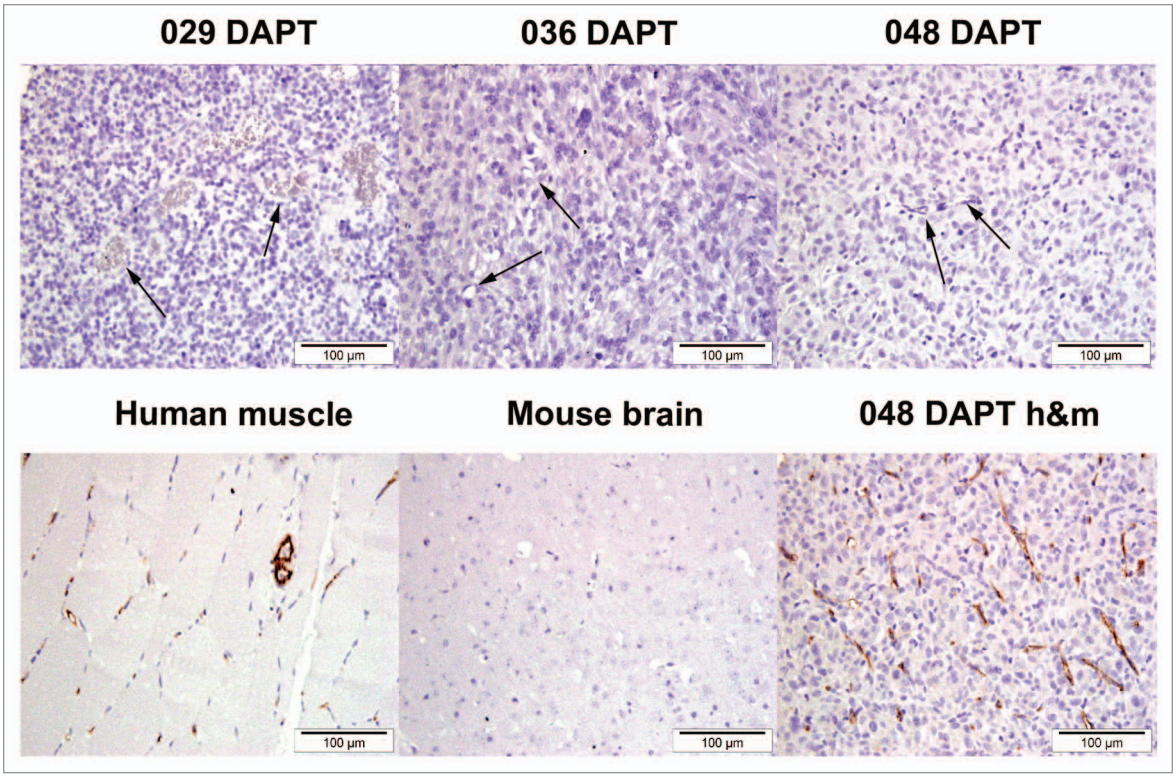

Figure 5. Intratumoral endothelial cells are not of human origin. Top row shows immunodetection of endothelial cells in tumors formed from DAPT-treated 029, 036, and 048 cells using a human-specific CD31 antibody. Arrows show negative endothelial cells. Bottom row shows immunodetection of the human-specific CD31 marker in a positive tissue control (human muscle) and a negative tissue control (mouse brain). 048 DAPT h&m is a section from the same tumor block as in the top row, but stained with a CD31 antibody detecting both human and mouse CD31.

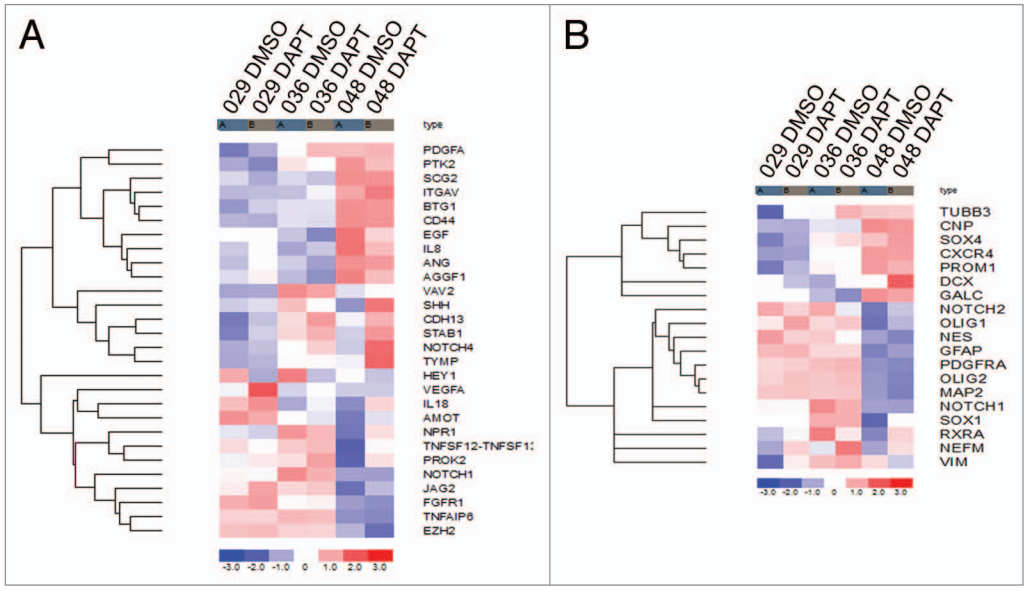

Figure 6. Gene expression of pro-angiogenic, NSC and differentiation markers. (**A**) Heat map showing the expression of selected pro-angiogenic markers in the 029, 036, and 048 neurosphere cultures treated with 10 µM DAPT or equal volumes of DMSO for 24 h. (**B**) Heat map showing the expression of selected markers of NSC (PROM1, NES, NOTCH1, NOTCH2, GFAP, CXCR4, SOX1, SOX4, PDGFRA, RXRA, and VIM), the neuronal linage (TUBB3, NEFM, MAP2, and DCX) and the glial lineage (GFAP, GALC, CNP, PDGFRA, VIM, OLIG1, and OLIG2) in the same samples as in (**A**). The colors represent the standard deviation in expression level relative to the mean expression of the respective gene across the six samples. Notice that some markers represent more than one phenotype, e.g., GFAP is a marker for both NSC and astrocytes.

upregulated in 048 upon DAPT treatment, while slightly downregulated in 029, suggesting that Hes-5 expression is regulated by different means in the two cultures. It is worth mentioning that embryonic Hes-5 knockouts are less severe than Hes-1 knockouts, indicating an inferior role for Hes-5 in NSC (reviewed in Fischer et al.[29]). The Notch-4 receptor has been implicated in the formation of mouse mammary tumors[30] and in maintenance of stem cells in breast cancer[31] and it has furthermore been suggested as a therapeutic target in triple negative breast cancers,[32] but the function of Notch-4 in GBM remains undetermined. Nevertheless, we found that the Notch-4 receptor was upregulated upon DAPT treatment in all three cultures. Together with the concomitant downregulation of the γ-secretase sub-unit PSENEN, one might speculate if signaling through the Notch-4 receptor could represent a redundant Notch pathway independent of γ-secreatase activity and thus a noncanonical pathway,[33] which would also explain why the Notch-4 high, Notch-1, -2, -3 low-expressing 048 culture seems almost unaffected by DAPT treatment on a functional level. One might argue that expression of PSENEN and the ADAM metalloprotease ADAM-17 in 048 further substantiates high Notch pathway activation. However, these are not exclusively modulators of Notch pathway activity, e.g., γ-secretase is also involved in the cleavage of among others the β-amyloid precursor protein (APP).[34] The high expression of PSENEN might even explain why so many transcripts are affected by DAPT treatment in the 048 culture, as additional γ-secretase targets in this culture has a greater potential to be affected. We also found the ligands DLL-1, -3, and Jagged-3 to be upregulated as a result of Notch inhibition in all three cultures which correlates with the process of lateral inhibition, where Notch signaling inhibits endogenous ligand expression.[12,13] It could be speculated why transcripts found to be similarly regulated between the cultures in the cluster analysis (**Fig. 1B**) are not represented in the differential expression analysis (**Table 1**). The explanation for this is the fold change cut off (≥1.3 or ≤–1.3) used in the latter analysis, e.g., DLL-1 upregulation does not seem to exceed 1.3 in either of the cultures when evaluated in the cluster analysis. In addition to known Notch pathway components (as seen in **Figure 1B**), several annotated transcripts were consistently regulated both between the 029 and 036 cultures and between all three (**Table 1**). Many of these transcripts were non-protein coding RNAs, such as ribosomal-, transfer-, and micro-RNAs, suggestive of further posttranscriptional regulation. Transcripts found to be upregulated in DAPT treated samples might be second line targets of Notch signaling, as first line targets, such as Hes-1 and Hey-1, tend to be transcriptional repressors.[29] Of the protein encoding transcripts upregulated in all three cultures, the cell adhesion molecules CEACAM5 and EPCAM have both been linked to migration, invasion and/or metastasis in numerous cancer types[35,36] and have further been associated with Notch signaling in human cervical cancers and pancreatic tumors, where Notch inhibition resulted in downregulation of CEACAM5 and EPCAM respectively.[37,38] A correlation between CEACAM5/EPCAM and Notch in GBM has yet to be reported. However, our results suggest that the correlation is in opposite as compared with cervical and pancreatic cancer as we found these

Table 3. Regulation of NSC and differentiation markers in DAPT treated samples compared with DMSO control

	NSC markers		Neuronal markers		Glial markers	
	Up	Down	Up	Down	Up	Down
29	SOX4	NES	TUBB3	DCX	OLIG1	
	PROM1	NOTCH2	NEFM			
	RXRA					
	VIM					
36	(SOX4)	NES	TUBB3		(OLIG1)	GALC
	(VIM)	NOTCH1	NEFM			
		NOTCH2	DCX			
		RXRA				
48	SOX4	PROM1	NEFM	(MAP2)	OLIG1	(GALC)
	NOTCH2	NES	DCX		GFAP	(OLIG2)
	SOX1	VIM				
	RXRA					
	GFAP					

Evaluation of markers of NSC, neuronal- and glial differentiation that are either up or downregulated in 029, 036, and 048 DAPT treated samples compared with control. Only markers that show a different expression level in the DAPT-treated samples compared with the control, as evaluated from **Figure 6B**, are presented in this table. Brackets symbolize that the regulation is minimal.

cell adhesion molecules to be upregulated upon Notch inhibition. Of the annotated transcripts found to be downregulated between all three cultures (apart from Hes-1 and Hey-1) were ephrin-B2 (EFNB2), GABA-B2 receptor (GABBR2), and eyes shut homolog (EYS) indicating them to be targets of active Notch signaling. Ephrin-B2 has been shown to be regulated by Notch signaling in human endothelial cells and during vascular development in zebrafish,[39,40] while no obvious correlation between EYS/GABA-B2 and Notch has been reported, although sequence homology has been identified between Notch-1 and a specific EYS splice variant (EYS/spacemaker [spam][41]). Thus further analyses are required to verify EYS and GABA-B2 as Notch targets, either direct or indirect, as the downregulation also could be the result of additional PSENEN targets, independent of Notch signaling.

When the cells were injected into the brains of SCID mice and allowed to form tumors, the histological appearance of the tumors also varied with the 029 and 036 tumors displaying a more diffuse and infiltrative growth pattern as compared with the 048 tumors that formed large, well bordered tumors. These observations could indicate that an endogenous high Notch activity leads to a more invasive and thus malignant phenotype. In line with this, it has been suggested that the level of Notch-1 expression increases with tumor grade in gliomas[42] and that Notch promotes migration and invasiveness of glioma cells, possibly through activation of β-catenin and NFκB signaling.[43] However, considering the fact that the 048 neurosphere cells formed tumors much faster than especially the 036 cells, one might speculate that the in vivo microenvironment ensures a faster establishment and growth of the 048 cells compared with

the 029 and in particular the 036 cells. This more rapid growth of the 048 cells might further cause the massive well-defined 048 tumors as a result of fast expansion of the tumor cells that displace the normal brain parenchyma simply by mass effect, while infiltrative growth, as observed in the 029 and 036 tumors, is a slower process due to degradation of tissue barriers. This is supported by observations that most 048 tumors were clearly detectable macroscopically both by the formation of a doomed head and by a heavily enlarged right hemisphere indicating a large mass within the brain that had dislocated the scalp, while mice injected with 029 and especially 036 cells, rarely displayed these objective signs of a tumor mass. The difference in survival time of mice injected with the three cultures, does, however, not match our previous in vitro observations[23] where the 029 and 036 cultures showed a fast and comparable growth pattern that was dissimilar to the slower growing 048 culture. It is recognized that the tumor microenvironment plays a fundamental role in the establishment, maintenance and growth of cancer cells in general[44] while the serum-free culture environment used in the present, and our previous study is known to support the growth and maintenance of NSC and bCSC.[9,10,45-48] It could as such be speculated that the 029 and 036 cultures are more stem cell-like and thus find better growth support in vitro than the 048 culture whose growth is better supported in vivo. Although the difference in Notch pathway signature between the cultures could support this hypothesis, it is purely speculation and additional studies are required to verify it.

We have previously shown that the 029 and 036 neurosphere cultures were sensitive to Notch inhibition as exemplified by reduced in vitro clonogenic growth potential upon pretreatment with the Notch inhibitor DAPT when compared with the DMSO control.[23] However, when the pretreated cells were injected into the brains of SCID mice, no increased survival was observed when compared with tumor formation from control treated cells. Thus pretreatment of the neurosphere cells with DAPT did not reduce tumor formation, indicating that it is not possible to eliminate all tumor forming cells by Notch inhibition. Surprisingly, DAPT treatment of the 036 cells actually seemed to decrease survival and led to a more rapid tumor formation when compared with the control treated 036 cells. Again the difference in microenvironment between in vitro and in vivo conditions should be considered. However, the discrepancy in treatment effect might also reflect the fact that, when we previously performed the in vitro clonogenic assay, we continued the treatment throughout the assay period, whereas when the cells were injected into the mice, DAPT was removed and the treatment ceased. Although Notch inhibition might not have been halted immediately after DAPT removal, it is most likely that Notch signaling was restored in vivo, which has also been observed by others.[18] The lack of positive effect from Notch treatment on survival is in contrast to previous reports in GBM-derived bCSC showing that GSI treatment prior to intracranial engraftment significantly prolonged survival of tumor-bearing mice.[18] Fan and colleagues suggested that this was due to ablation of bCSC by Notch inhibition. They did, however, not observe any histological difference between treatment and control groups by microscopically evaluation of H&E brain sections.[18] This is in contrast to our observations as we found that DAPT treatment of especially the 036 neurosphere cells resulted in tumors with large voluminous vessels. When evaluating the endothelial cell marker CD31 we found that these vessels tended to be disorganized and abnormal. It has been demonstrated that bCSC can transdifferentiate into endothelial cells,[49] and an intriguing thought might be that Notch inhibition induces differentiation of at least some of the bCSC down an alternative lineage, namely toward endothelial cells. However, we did not find the endothelial cells to be of human origin, why we suggest that ex vivo Notch inhibition in neurosphere cells with high endogenous Notch activity merely selects for a cell type that more strongly induces angiogenesis in vivo. This notion is supported by our gene expression analysis were we found the essential pro-angiogenic growth factors VEGFA and PDGFA to be upregulated only in 029 and 036, and additional pro-angiogenic factors (CDH13, STAB1, and IL18) upregulated in all three cultures. Moreover, we found that the Notch ligand DLL-4 was upregulated in the DAPT treated samples, and it has been demonstrated that glioma cells expressing DLL-4 activates Notch signaling in the host stromal/endothelial cells increasing vessel size and improving vascular function in the tumor,[50] which is in line with the large vessels we observed in some of our DAPT tumors. The link between Notch-DLL4 signaling and angiogenesis is well known, and inhibition of DLL-4 has been suggested to hamper tumor growth by inducing non-functional small vessels[51-53] and Notch inhibition has been shown to abolish DLL-4-mediated resistance to anti-angiogenic treatment.[54] It should be emphasized that the IHC and the gene expression analyses cannot be directly compared, as the IHC data represents the expression of selected markers in pre-treated neurosphere cells after in vivo tumor formation, whereas the gene expression data was evaluated after 24 h of in vitro treatment of the neurosphere cultures. Nevertheless, some of the results are supportive of one another, such as the low expression of Notch-1 in 048 and the downregulation of Nestin upon DAPT treatment.

It has been shown that the Notch pathway is essential for maintaining the undifferentiated phenotype of normal neural stem cells and that inhibition of the pathway leads to differentiation.[55-57] If active Notch signaling in the same way plays a role in maintenance of the immature state of the bCSC population in the culture but is not essential for the growth of GBM neurosphere cells in vivo, one might speculate that Notch inhibition merely leads to differentiation of the bCSC cells as previously has been demonstrated,[16,17,58] rather than killing them as others have suggested.[18] In line with this, it has been demonstrated that some GSIs, including DAPT, are unable to kill bCSC.[59] As such, it could be speculated that the DAPT treatment in our study targeted the bCSC population by differentiating them and as such, the cells injected into mice were more differentiated progenitor cells that were still able to expand and form tumors. This was supported by a downregulation of Nestin mRNA after 24 h of in vitro DAPT treatment and decreased levels of Nestin in a subset of 029 and 036 tumors established from DAPT-treated cultures, as evaluated by IHC. This decrease of Nestin-positive cells upon Notch inhibition has also been reported in vitro[58] and

Nestin has moreover been proposed as a direct transcriptional target of the Notch pathway in GBM.[60] Furthermore, in the case of 036, the DMSO tumors displayed fewer proliferating cells than the DAPT-treated tumors, which correlates with a faster proliferation of progenitor cells compared with more immature stem cells.[61-63] When evaluating the expression of additional NSC and differentiation markers we found that especially the 036 culture showed downregulation of the stem cell markers and upregulation of the neuronal markers upon DAPT treatment. These results indicate that the 036 cells have begun differentiating toward the neuronal lineage upon inhibition of Notch signaling, in line with the known function of Notch in normal NSC[55-57] and the high expression of DLL-3 and -4 in this culture. In the 029 culture, upregulation of neuronal markers also tended to predominate while the 048 culture did not show a clear differentiation picture, again suggesting that the effect from Notch inhibition in this culture differs from the effect in 029 and 036. Taken together, these data suggest that Notch inhibition by DAPT treatment in cultures with an elevated Notch pathway signature leads to a more neuronal phenotype with a higher proliferative index, abnormal vasculature and perhaps even decreased survival. Apart from differentiation, these are all indications of the Notch pathway being a tumor suppressor. Indeed it has been demonstrated that Notch is considered a tumor suppressor in different cancer types, as exemplified in the embryonal brain tumor medulloblastoma. Here Notch-1 and Notch-2 were demonstrated to have opposite effects with Notch-1 acting as a tumor suppressor and Notch-2 as an oncogene.[64] However, GSI treatment targets all four Notch receptors, and as such it is not possible in our study to reveal the function of the individual Notch receptors. Moreover, if inhibition of Notch signaling partly induces differentiation of the bCSC population into faster proliferating progenitor cells and if considering the implications that bCSC can be accounted for the chemo- and radio-resistance seen in GBM patients, maybe a combination of traditional therapy targeting the highly proliferative cancer cells together with Notch inhibition that differentiate and thus sensitize the bCSC population to the traditional treatment[65] would be feasible. However, this is highly speculative and future studies will need to verify this hypothesis. Nevertheless, based on the results of this study, we believe that the Notch signaling pathway presents a potential target for future anti-bCSC treatment and that a regimen that includes Notch inhibition would improve the therapy for GBM patients displaying an elevated Notch pathway signature.

In conclusion, this study demonstrates that GBM-derived neurosphere cultures can be assigned a distinguished Notch pathway signature based on global gene expression analysis, and that cultures with high Notch expression tended to form intracranial tumors with a more infiltrative growth pattern. However, there was no survival benefit when the mice were injected with cultures treated with a Notch inhibitor prior to engraftment when compared with the control treatment, regardless of culture Notch pathway signature. We did nevertheless find indications that Notch inhibition lead to differentiation and increased angiogenic potential, both in vivo and in vitro, in GBM cultures defined as having high endogenous Notch pathway activation. Based on the presented results we therefore suggest that bCSC targeted anti-Notch treatment in combination with traditional therapy might be feasible in patient with an elevated Notch pathway signature, as Notch inhibition possibly induces the bCSC population to differentiate and thereby sensitizes them to chemo- and radiation therapy.

Materials and Methods

GBM neurosphere cultures

Establishment and characterization of the neurosphere cultures used in this study has previously been described.[23,24] In short, neurosphere cultures were established from acutely dissociated patient-derived subcutaneous xenograft tumors and maintained in NB-media (Neurobasal-A media supplemented with 1× B-27 Supplement, 1× L-glutamine, 10 ng/mL Basic Fibroblastic Growth Factor [bFGF], 10 ng/mL Epidermal Growth Factor [EGF], 1% Pen Strep [penicillin–streptomycin] [all from Invitrogen] and 10 ng/mL Leukemia Inhibitory Factor [LIF, Chemicon]). The cells were cultivated in cell culture flasks (Nunc) in a humidified chamber with 5% CO_2 at 37 °C. Fresh media was added twice a week and spheres were mechanically dissociated at every passage. Neurosphere cultures used in the present study were: GBM_CPH029p7, NGBM_CPH036p7, and NGBM_CPH048p6. pX indicates the xenograft mouse passage from which the individual cultures were established. The prefix "N" refers to that the xenograft has been transplanted onto nude rats for a period to remove mouse hepatitis infection. For simplicity, the cultures have been designated 029, 036, and 048 respectively. It is necessary to comment on that after having concluded the experiments for this and previously published studies,[23,24] we did a Short Tandem Repeat (STR)-profile of all our in vitro established neurosphere cultures. In that context we found that the profile of the GBM_CPH029p7 (xenograft passage 7) culture showed great similarity to neurosphere cultures established from (N)GBM_CPH036pX xenografts. As such, it is most likely that the 029 culture is derived from a 036 xenograft tumor and thus the original GBM_CPH036 patient tumor.[23,24] However, as the 029 and 036 cultures have been cultured separately since they were established in 2007 and 2008 respectively, we have chosen to treat them as two individual cultures. Nevertheless, it should be held in mind that they most likely originate from the same patient tumor.

Preparation of samples for microarray analysis

Neurosphere cells were dissociated and 1–1.5 × 10^6 cells were plated in 10 mL NB-media in a petri dish (10 cm Ø, Nunc) and treated the next day with 10 μM DAPT (N-[N-(3,5-Difluorophenacetyl-L-alanyl)]-S-phenylglycine *t*-Butyl Ester (γ-secretase inhibitor [GSI] IX, Calbiochem) dissolved in dimethyl-sulfoxide [DMSO] hybri-max [Sigma]), equal volumes of DMSO for control or left untreated. Twenty-four hours after treatment initiation the cells were harvested and total RNA was extracted from cell pellets using QIAshredder columns and RNeasy Mini KIT (both from Qiagen) according to manufacturers' protocol. All

RNA was DNase treated using the RNase-Free DNase Set from Qiagen.

Microarray analysis

RNA was amplified and biotin-labeled using the Ambion WT Expression Kit (Applied Biosystems) according to manufacturers' instructions. Two-hundredy fifty nanograms total RNA was used as input. The labeled samples were hybridized to the Human Gene 1.0 ST GeneChip array (Affymetrix). The arrays were washed and stained with phycoerytrin conjugated streptavidin (SAPE) using the Affymetrix Fluidics Station® 450, and the arrays were scanned in the Affymetrix GeneArray® 3000 scanner to generate fluorescent images, as described in the Affymetrix GeneChip® protocol. Cell intensity (CEL) files were generated in the GeneChip Command Console Software (AGCC) (Affymetrix). The CEL files were imported into the PARTEK software and normalized using the RMA (Robust Multi-array Average) method including background correction, quantile normalization and probe set summarization to provide each transcript with a single expression value.

Hierarchical cluster visualization of predefined gene lists

Gene lists of biological interest were downloaded from the Molecular signatures Database v. 3.1 from the Broad Institute (MSigDB, http://www.broadinstitute.org/gsea/msigdb/index.jsp). Notch pathway components as well as pro-angiogenic-, NSC-, and differentiation markers were further selected based on the http://www.genecards.org and the http://www.ncbi.nlm.nih.gov/pubmed websites. Overlap between the downloaded gene lists and the probe sets on the microarray was generated using the NetAffx database and based on overlap in gene symbol between annotated probe sets on the microarray and the gene list. Hierarchical cluster visualization was performed using dChip using Euclidean distance and average linkage clustering.

Differential expression analysis

Group comparisons were performed by comparing each treated culture sample to its own control and differentially expressed transcripts were defined as having a fold change ≥1.3 or ≤–1.3 between DMSO control and DAPT-treated sample, based on the fold change of Hes-1 and Hey-1. Transcripts that were consistently regulated across the three cultures were visualized in a Venn diagram displaying the transcripts that were either up- or downregulated for each comparison. Only transcripts with an annotation are presented in the Venn diagram. A paired *t* test ($n = 3$, $P < 0.05$) was performed between control and treated group samples in order to define if the regulation of the annotated transcript was significant.

Intracranial growth of GBM neurosphere cells

Neurosphere cells were dissociated and 3×10^6 cells were plated in 25 mL NB-media in a culture flask (Nunc). DAPT was added the following day at a concentration of 10 μM and equal volume of DMSO was added to the control. After seven days of treatment the cells were harvested by centrifugation (300× g), mechanically dissociated and re-suspended in warm NB-media at 10000 cells/μL. Parallel cell pellets were harvested and snap frozen in liquid N_2 for protein analysis (see below). Ten microliter cell suspension (100000 cells) was injected into the brains of 6- to 9-wk-old female C.B-17 SCID mice: The mouse was anesthetized by i.p. administration of Hypnorm-Midazolam (1 mL/100 g body weight) and the head was fixed in a stereotactic frame (KOPF model 963, 926-B, and 922: Better Hospital Equipment Corp). A short longitudinal incision was made in the scalp exposing the calvarium. Using a micro-drill, a burr-hole was made in the skull 1.5 mm right of the sutura sagittalis and 0.5 mm posterior to bregma. GBM neurosphere cells were injected at the depth of 2.0–2.5 mm at a rate of 60 nL/sec using a 100 μL syringe with a 25-gauge needle (SGE100RN: World Precision Instruments) placed in a microinfusion pump (Micro 4 pump and MicroSyringePump Controller: World Precision Instruments and KOPF model 1770-C: Better Hospital Equipment Corp). When injection was finished the needle was withdrawn after 1 min. Bupivacain (0.2 mg/100 g body weight) and Lidocain (1 mg/100 g body weight) were administrated in the incision site for local anesthetic before the skin was closed with an Ethicon 5–0 prolene suture. A total of seven mice were injected in each group and tumor formation was monitored by frequent ocular observation and weighing the animals. One to three randomly selected mice from each group were subjected to in situ tumor visualization by small animal PET/CT scanning using ^{18}F-FET as a tracer (PET, positron emission tomography; CT, X-ray computer tomography; ^{18}F-FET, *O*-(2-[^{18}F]fluoroethyl)-L-tyrosine).[66] The scanning was performed under Hypnorm-Midazolam anesthesia: mice were injected i.v. with approximately 10 MBq ^{18}F-FET. Twenty minutes after tracer injection a 10 min PET scan was acquired using a MicroPET Focus 120 (Siemens Medical Solutions). PET data were arranged into sinograms and subsequently reconstructed with the maximum a posteriori (MAP) reconstruction algorithm. The pixel size was 0.866 × 0.866 × 0.796 mm and the resolution was 1.4 mm full-width-at-half-maximum. Following the microPET scan, a 7 min and 10 s microCT scan was acquired with a MicroCATH II system (Siemens Medical Solutions) with the following parameter settings: 360 rotation steps, tube voltage 60 kV, tube current 500 mA, binning 4, and exposure time 310 ms. The pixel size was 0.091 × 0.091 × 0.091 mm. PET and microCT images were fused in the Inveon software (Siemens Medical Solutions). The mice used for in situ visualization could not be included in the survival data, as they did not tolerate the weekly sedation well, and as survival was used as the primary endpoint in this study. Mice were humanly euthanized when they showed tumor related symptoms such as a hunched position, bristly and greasy fur, lethargy, neurological signs, and/or weight loss. Subsequently the brains were gently removed from the cranial cavity and fixed in 4% paraformaldehyde that after 24 h was exchanged for 70% EtOH. For immunohistochemical (IHC) analysis the brains were sliced by coronally cutting the brain in the incision site and embedding the pieces in paraffin. From the block anterior to the incision site, 4 μm histological sections were prepared for IHC (see below).

Protein purification and western blotting

Whole cell lysates were prepared from cell pellets by sonication in ice-cold RIPA buffer (50 mM Tris-HCL [pH 7.4], 1% NP40, 0.25% Na-deoxycholate, 150 mM NaCl, 1 mM EDTA) supplemented with protease and phosphatase inhibitor mixture II and III (Calbiochem). Protein concentrations were determined

using the BCA protein assay (Pierce) according to manufacturers' instructions. For western blotting (WB) 50 μg protein was separated on 4–12% NuPAGE Bis-Tris gels and electroblotted onto nitrocellulose membranes (both from Invitrogen) according to manufacturers' protocol. The membranes were then blocked for 1 h in 5% non-fat milk at room temperature (RT) and incubated with primary antibody diluted in 5% non-fat milk ON at 4 °C, followed by horseradish peroxidase (HRP) conjugated secondary antibodies for 1 h at RT. Blots were developed using the SuperSignal West Dura Extended Duration Substrate (Thermo Scientific) and the UVP, BioSpectrum® AC Imaging System and VisionWorks®LS software (UVP). Primary antibodies: Goat polyclonal anti Notch-1 [S-20] (diluted 1:100, Santa Cruz sc-23304), Rabbit polyclonal anti Hes-1 (diluted 1:2000, kindly provided by Dr Tetsou Sudo, Toray Industries Inc.) and Rabbit monoclonal anti α-Tubulin [11H10] (diluted 1:1000, Cell Signaling 2125). Secondary antibodies: Rabbit polyclonal anti goat IgG (diluted 1:2000, Dako P0217) and Swine polyclonal anti rabbit IgG (diluted 1:1000, Dako P0449).

Immunohistochemistry

Immunohistochemistry (IHC) was performed on formalin-fixed, paraffin-embedded tissue. For each of the three tumor-types (029, 036, and 048) in each of the two treatment groups (DMSO and DAPT), we stained histological sections (4 μM) from three different mice with hematoxylin and eosin (H&E) for normal histological evaluation and with antibodies detecting different molecular markers as described below. All IHC stainings were performed manually. Briefly, formalin-fixed and paraffin-embedded slides were heated for 1 h at 60 °C, followed by deparaffination in xylene and rehydration. Endogenous peroxidase activity was quenched by treating with 0.3% hydrogen-peroxide in water for 30 min. Antigen retrieval was performed by immersing the sections in water bath containing citrate buffer (DAKO) for 30 min at 95 °C. Subsequently, the slides were blocked for 20 min in PBS with 2% horse serum before incubation with primary antibody diluted in blocking buffer over night at 4 °C followed by biotinylated universal secondary antibody (anti-rabbit and -mouse IgG) and horseradish peroxidase (HRP) conjugated Avidin/Biotin Complex (ABC) reagent (secondary antibody and ABC reagent were both diluted 1:50 and incubated for 30–60 min at RT, Vector Kit PK-6200). The signal was developed by Diaminobenzidine (DAB, BioGenex HK153-5KE) for 5 min. Finally the sections were counterstained with Mayer's hematoxylin, dehydrated with increasing concentrations of ethanol and mounted with DPX (Sigma-Aldrich). Primary antibodies used: Nestin (diluted 1:10 000, Millipore NG1853940), Notch-1 (diluted 1:200, Cell Signaling 3608), CD31 (detecting both human and murine CD31, diluted 1:50, Abcam ab28364), CD31 (detecting only human CD31, diluted 1:100, Abcam ab76533) and Ki-67 (diluted 1:100, Abcam ab8191). Light microscopy of the IHC sections was performed using the Olympus BX51 microscope, the Olympus D71 camera and the Cell^A 2.5 (Build 1163) Olympus Soft Imaging Solutions GmbH software.

Ethics statement

In a previous study[24] patient GBM material was obtained from surgery at Copenhagen University Hospital, Denmark, approved by the Scientific Ethical Committee for Copenhagen and Frederiksberg: (KF) 01-034/04 with the patients' informed consent. All animal experiments were performed according to Danish legislation.

Disclosure of Potential Conflict of Interest

The authors declare that they have no competing interests.

Acknowledgments

We thank Babloo Lukram for performing the immunohistochemistry and the Department of Neuropathology for technical assistance and advice. Financial support was kindly provided by: The Faculty of Health Sciences, University of Copenhagen (211-0610/09-3012); Dansk Kraeftforsknings Fond; Kong Christian den Tiendes Fond; Civilingenioer Frode V. Nyegaard og Hustrus Fond, Harboefonden, Danish National Advanced Technology Foundation, and The AP Møller Foundation.

Supplemental Materials

Supplemental materials may be found here:
www.landesbioscience.com/journals/cbt/article/28876/

References

1. Ohgaki H, Kleihues P. Population-based studies on incidence, survival rates, and genetic alterations in astrocytic and oligodendroglial gliomas. J Neuropathol Exp Neurol 2005; 64:479-89; PMID:15977639
2. Filippini G, Falcone C, Boiardi A, Broggi G, Bruzzone MG, Caldiroli D, Farina R, Farinotti M, Fariselli L, Finocchiaro G, et al.; Brain Cancer Register of the Fondazione IRCCS (Istituto Ricovero e Cura a Carattere Scientifico) Istituto Neurologico Carlo Besta. Prognostic factors for survival in 676 consecutive patients with newly diagnosed primary glioblastoma. Neuro Oncol 2008; 10:79-87; PMID:17993634; http://dx.doi.org/10.1215/15228517-2007-038
3. Lathia JD, Gallagher J, Myers JT, Li M, Vasanji A, McLendon RE, Hjelmeland AB, Huang AY, Rich JN. Direct in vivo evidence for tumor propagation by glioblastoma cancer stem cells. PLoS One 2011; 6:e24807; PMID:21961046; http://dx.doi.org/10.1371/journal.pone.0024807
4. Bao S, Wu Q, McLendon RE, Hao Y, Shi Q, Hjelmeland AB, Dewhirst MW, Bigner DD, Rich JN. Glioma stem cells promote radioresistance by preferential activation of the DNA damage response. Nature 2006; 444:756-60; PMID:17051156; http://dx.doi.org/10.1038/nature05236
5. Bao S, Wu Q, Sathornsumetee S, Hao Y, Li Z, Hjelmeland AB, Shi Q, McLendon RE, Bigner DD, Rich JN. Stem cell-like glioma cells promote tumor angiogenesis through vascular endothelial growth factor. Cancer Res 2006; 66:7843-8; PMID:16912155; http://dx.doi.org/10.1158/0008-5472.CAN-06-1010
6. Liu G, Yuan X, Zeng Z, Tunici P, Ng H, Abdulkadir IR, Lu L, Irvin D, Black KL, Yu JS. Analysis of gene expression and chemoresistance of CD133+ cancer stem cells in glioblastoma. Mol Cancer 2006; 5:67; PMID:17140455; http://dx.doi.org/10.1186/1476-4598-5-67
7. Huang Q, Zhang QB, Dong J, Wu YY, Shen YT, Zhao YD, Zhu YD, Diao Y, Wang AD, Lan Q. Glioma stem cells are more aggressive in recurrent tumors with malignant progression than in the primary tumor, and both can be maintained long-term in vitro. BMC Cancer 2008; 8:304; PMID:18940013; http://dx.doi.org/10.1186/1471-2407-8-304
8. Mariani CL, Kouri JG, Streit WJ. Rejection of RG-2 gliomas is mediated by microglia and T lymphocytes. J Neurooncol 2006; 79:243-53; PMID:16612573; http://dx.doi.org/10.1007/s11060-006-9137-x
9. Ignatova TN, Kukekov VG, Laywell ED, Suslov ON, Vrionis FD, Steindler DA. Human cortical glial tumors contain neural stem-like cells expressing astroglial and neuronal markers in vitro. Glia 2002; 39:193-206; PMID:12203386; http://dx.doi.org/10.1002/glia.10094
10. Singh SK, Clarke ID, Terasaki M, Bonn VE, Hawkins C, Squire J, Dirks PB. Identification of a cancer stem cell in human brain tumors. Cancer Res 2003; 63:5821-8; PMID:14522905

11. Singh SK, Hawkins C, Clarke ID, Squire JA, Bayani J, Hide T, Henkelman RM, Cusimano MD, Dirks PB. Identification of human brain tumour initiating cells. Nature 2004; 432:396-401; PMID:15549107; http://dx.doi.org/10.1038/nature03128
12. Chiba S. Notch signaling in stem cell systems. Stem Cells 2006; 24:2437-47; PMID:16888285; http://dx.doi.org/10.1634/stemcells.2005-0661
13. Beatus P, Lendahl U. Notch and neurogenesis. J Neurosci Res 1998; 54:125-36; PMID:9788272; http://dx.doi.org/10.1002/(SICI)1097-4547(19981015)54:2<125::AID-JNR1>3.0.CO;2-G
14. Margareto J, Leis O, Larrarte E, Idoate MA, Carrasco A, Lafuente JV. Gene expression profiling of human gliomas reveals differences between GBM and LGA related to energy metabolism and notch signaling pathways. J Mol Neurosci 2007; 32:53-63; PMID:17873288; http://dx.doi.org/10.1007/s12031-007-0008-5
15. Lee J, Kotliarova S, Kotliarov Y, Li A, Su Q, Donin NM, Pastorino S, Purow BW, Christopher N, Zhang W, et al. Tumor stem cells derived from glioblastomas cultured in bFGF and EGF more closely mirror the phenotype and genotype of primary tumors than do serum-cultured cell lines. Cancer Cell 2006; 9:391-403; PMID:16697959; http://dx.doi.org/10.1016/j.ccr.2006.03.030
16. Purow BW, Haque RM, Noel MW, Su Q, Burdick MJ, Lee J, Sundaresan T, Pastorino S, Park JK, Mikolaenko I, et al. Expression of Notch-1 and its ligands, Delta-like-1 and Jagged-1, is critical for glioma cell survival and proliferation. Cancer Res 2005; 65:2353-63; PMID:15781650; http://dx.doi.org/10.1158/0008-5472.CAN-04-1890
17. Hu YY, Zheng MH, Cheng G, Li L, Liang L, Gao F, Wei YN, Fu LA, Han H. Notch signaling contributes to the maintenance of both normal neural stem cells and patient-derived glioma stem cells. BMC Cancer 2011; 11:82; PMID:21342503; http://dx.doi.org/10.1186/1471-2407-11-82
18. Fan X, Khaki L, Zhu TS, Soules ME, Talsma CE, Gul N, Koh C, Zhang J, Li YM, Maciaczyk J, et al. NOTCH pathway blockade depletes CD133-positive glioblastoma cells and inhibits growth of tumor neurospheres and xenografts. Stem Cells 2010; 28:5-16; PMID:19904829
19. Verhaak RG, Hoadley KA, Purdom E, Wang V, Qi Y, Wilkerson MD, Miller CR, Ding L, Golub T, Mesirov JP, et al.; Cancer Genome Atlas Research Network. Integrated genomic analysis identifies clinically relevant subtypes of glioblastoma characterized by abnormalities in PDGFRA, IDH1, EGFR, and NF1. Cancer Cell 2010; 17:98-110; PMID:20129251; http://dx.doi.org/10.1016/j.ccr.2009.12.020
20. Bezwoda WR, Derman D, De Moor NG, Lange M, Levin J. Treatment of metastatic breast cancer in estrogen receptor positive patients. A randomized trial comparing tamoxifen alone versus tamoxifen plus CMF. Cancer 1982; 50:2747-50; PMID:6754067; http://dx.doi.org/10.1002/1097-0142(19821215)50:12<2747::AID-CNCR2820501209>3.0.CO;2-Y
21. Marty M, Cognetti F, Maraninchi D, Snyder R, Mauriac L, Tubiana-Hulin M, Chan S, Grimes D, Antón A, Lluch A, et al. Randomized phase II trial of the efficacy and safety of trastuzumab combined with docetaxel in patients with human epidermal growth factor receptor 2-positive metastatic breast cancer administered as first-line treatment: the M77001 study group. J Clin Oncol 2005; 23:4265-74; PMID:15911866; http://dx.doi.org/10.1200/JCO.2005.04.173
22. Andersen J, Poulsen HS. Immunohistochemical estrogen receptor determination in paraffin-embedded tissue. Prediction of response to hormonal treatment in advanced breast cancer. Cancer 1989; 64:1901-8; PMID:2790701; http://dx.doi.org/10.1002/1097-0142(19891101)64:9<1901::AID-CNCR2820640924>3.0.CO;2-W
23. Kristoffersen K, Villingshøj M, Poulsen HS, Stockhausen MT. Level of Notch activation determines the effect on growth and stem cell-like features in glioblastoma multiforme neurosphere cultures. Cancer Biol Ther 2013; 14:625-37; PMID:23792644; http://dx.doi.org/10.4161/cbt.24595
24. Stockhausen MT, Broholm H, Villingshøj M, Kirchhoff M, Gerdes T, Kristoffersen K, Kosteljanetz M, Spang-Thomsen M, Poulsen HS. Maintenance of EGFR and EGFRvIII expressions in an in vivo and in vitro model of human glioblastoma multiforme. Exp Cell Res 2011; 317:1513-26; PMID:21514294; http://dx.doi.org/10.1016/j.yexcr.2011.04.001
25. Phillips HS, Kharbanda S, Chen R, Forrest WF, Soriano RH, Wu TD, Misra A, Nigro JM, Colman H, Soroceanu L, et al. Molecular subclasses of high-grade glioma predict prognosis, delineate a pattern of disease progression, and resemble stages in neurogenesis. Cancer Cell 2006; 9:157-73; PMID:16530701; http://dx.doi.org/10.1016/j.ccr.2006.02.019
26. Brennan C, Momota H, Hambardzumyan D, Ozawa T, Tandon A, Pedraza A, Holland E. Glioblastoma subclasses can be defined by activity among signal transduction pathways and associated genomic alterations. PLoS One 2009; 4:e7752; PMID:19915670; http://dx.doi.org/10.1371/journal.pone.0007752
27. Hegi ME, Diserens AC, Gorlia T, Hamou MF, de Tribolet N, Weller M, Kros JM, Hainfellner JA, Mason W, Mariani L, et al. MGMT gene silencing and benefit from temozolomide in glioblastoma. N Engl J Med 2005; 352:997-1003; PMID:15758010; http://dx.doi.org/10.1056/NEJMoa043331
28. Henrique D, Hirsinger E, Adam J, Le Roux I, Pourquié O, Ish-Horowicz D, Lewis J. Maintenance of neuroepithelial progenitor cells by Delta-Notch signalling in the embryonic chick retina. Curr Biol 1997; 7:661-70; PMID:9285721; http://dx.doi.org/10.1016/S0960-9822(06)00293-4
29. Fischer A, Gessler M. Delta-Notch--and then? Protein interactions and proposed modes of repression by Hes and Hey bHLH factors. Nucleic Acids Res 2007; 35:4583-96; PMID:17586813; http://dx.doi.org/10.1093/nar/gkm477
30. Raafat A, Lawson S, Bargo S, Klauzinska M, Strizzi L, Goldhar AS, Buono K, Salomon D, Vonderhaar BK, Callahan R. Rbpj conditional knockout reveals distinct functions of Notch4/Int3 in mammary gland development and tumorigenesis. Oncogene 2009; 28:219-30; PMID:18836481; http://dx.doi.org/10.1038/onc.2008.379
31. Harrison H, Farnie G, Howell SJ, Rock RE, Stylianou S, Brennan KR, Bundred NJ, Clarke RB. Regulation of breast cancer stem cell activity by signaling through the Notch4 receptor. Cancer Res 2010; 70:709-18; PMID:20068161; http://dx.doi.org/10.1158/0008-5472.CAN-09-1681
32. Speiser J, Foreman K, Drinka E, Godellas C, Perez C, Salhadar A, Erşahin Ç, Rajan P. Notch-1 and Notch-4 biomarker expression in triple-negative breast cancer. Int J Surg Pathol 2012; 20:139-45; PMID:22084425; http://dx.doi.org/10.1177/1066896911427035
33. Gentle ME, Rose A, Bugeon L, Dallman MJ. Noncanonical Notch signaling modulates cytokine responses of dendritic cells to inflammatory stimuli. J Immunol 2012; 189:1274-84; PMID:22753939; http://dx.doi.org/10.4049/jimmunol.1103102
34. Evin G, Cappai R, Li QX, Culvenor JG, Small DH, Beyreuther K, Masters CL. Candidate gamma-secretases in the generation of the carboxyl terminus of the Alzheimer's disease beta A4 amyloid: possible involvement of cathepsin D. Biochemistry 1995; 34:14185-92; PMID:7578016; http://dx.doi.org/10.1021/bi00043a024
35. Blumenthal RD, Hansen HJ, Goldenberg DM. Inhibition of adhesion, invasion, and metastasis by antibodies targeting CEACAM6 (NCA-90) and CEACAM5 (Carcinoembryonic Antigen). Cancer Res 2005; 65:8809-17; PMID:16204051; http://dx.doi.org/10.1158/0008-5472.CAN-05-0420
36. Patriarca C, Macchi RM, Marschner AK, Mellstedt H. Epithelial cell adhesion molecule expression (CD326) in cancer: a short review. Cancer Treat Rev 2012; 38:68-75; PMID:21576002; http://dx.doi.org/10.1016/j.ctrv.2011.04.002
37. Bajaj J, Maliekal TT, Vivien E, Pattabiraman C, Srivastava S, Krishnamurthy H, Giri V, Subramanyam D, Krishna S. Notch signaling in CD66+ cells drives the progression of human cervical cancers. Cancer Res 2011; 71:4888-97; PMID:21646470; http://dx.doi.org/10.1158/0008-5472.CAN-11-0543
38. Palagani V, El Khatib M, Kossatz U, Bozko P, Müller MR, Manns MP, Krech T, Malek NP, Plentz RR. Epithelial mesenchymal transition and pancreatic tumor initiating CD44+/EpCAM+ cells are inhibited by γ-secretase inhibitor IX. PLoS One 2012; 7:e46514; PMID:23094026; http://dx.doi.org/10.1371/journal.pone.0046514
39. Shawber CJ, Das I, Francisco E, Kitajewski J. Notch signaling in primary endothelial cells. Ann N Y Acad Sci 2003; 995:162-70; PMID:12814948; http://dx.doi.org/10.1111/j.1749-6632.2003.tb03219.x
40. Lawson ND, Scheer N, Pham VN, Kim CH, Chitnis AB, Campos-Ortega JA, Weinstein BM. Notch signaling is required for arterial-venous differentiation during embryonic vascular development. Development 2001; 128:3675-83; PMID:11585794
41. Isackson PJ, Ochs-Balcom HM, Ma C, Harley JB, Peltier W, Tarnopolsky M, Sripathi N, Wortmann RL, Simmons Z, Wilson JD, et al. Association of common variants in the human eyes shut ortholog (EYS) with statin-induced myopathy: evidence for additional functions of EYS. Muscle Nerve 2011; 44:531-8; PMID:21826682; http://dx.doi.org/10.1002/mus.22115
42. Xu P, Yu S, Jiang R, Kang C, Wang G, Jiang H, Pu P. Differential expression of Notch family members in astrocytomas and medulloblastomas. Pathol Oncol Res 2009; 15:703-10; PMID:19424825; http://dx.doi.org/10.1007/s12253-009-9173-x
43. Zhang X, Chen T, Zhang J, Mao Q, Li S, Xiong W, Qiu Y, Xie Q, Ge J. Notch1 promotes glioma cell migration and invasion by stimulating β-catenin and NF-κB signaling via AKT activation. Cancer Sci 2012; 103:181-90; PMID:22093097; http://dx.doi.org/10.1111/j.1349-7006.2011.02154.x
44. Jandial R, U H, Levy ML, Snyder EY. Brain tumor stem cells and the tumor microenvironmen. Neurosurg Focus 2008; 24:E27; PMID:18341404; http://dx.doi.org/10.3171/FOC/2008/24/3-4/E26
45. Reynolds BA, Weiss S. Generation of neurons and astrocytes from isolated cells of the adult mammalian central nervous system. Science 1992; 255:1707-10; PMID:1553558; http://dx.doi.org/10.1126/science.1553558
46. Gritti A, Parati EA, Cova L, Frolichsthal P, Galli R, Wanke E, Faravelli L, Morassutti DJ, Roisen F, Nickel DD, et al. Multipotential stem cells from the adult mouse brain proliferate and self-renew in response to basic fibroblast growth factor. J Neurosci 1996; 16:1091-100; PMID:8558238
47. Gritti A, Frölichsthal-Schoeller P, Galli R, Parati EA, Cova L, Pagano SF, Bjornson CR, Vescovi AL. Epidermal and fibroblast growth factors behave as mitogenic regulators for a single multipotent stem cell-like population from the subventricular region of the adult mouse forebrain. J Neurosci 1999; 19:3287-97; PMID:10212288

48. Galli R, Binda E, Orfanelli U, Cipelletti B, Gritti A, De Vitis S, Fiocco R, Foroni C, Dimeco F, Vescovi A. Isolation and characterization of tumorigenic, stem-like neural precursors from human glioblastoma. Cancer Res 2004; 64:7011-21; PMID:15466194; http://dx.doi.org/10.1158/0008-5472.CAN-04-1364
49. He H, Niu CS, Li MW. Correlation between glioblastoma stem-like cells and tumor vascularization. Oncol Rep 2012; 27:45-50; PMID:21971709
50. Li JL, Sainson RC, Shi W, Leek R, Harrington LS, Preusser M, Biswas S, Turley H, Heikamp E, Hainfellner JA, et al. Delta-like 4 Notch ligand regulates tumor angiogenesis, improves tumor vascular function, and promotes tumor growth in vivo. Cancer Res 2007; 67:11244-53; PMID:18056450; http://dx.doi.org/10.1158/0008-5472.CAN-07-0969
51. Noguera-Troise I, Daly C, Papadopoulos NJ, Coetzee S, Boland P, Gale NW, Lin HC, Yancopoulos GD, Thurston G. Blockade of Dll4 inhibits tumour growth by promoting non-productive angiogenesis. Nature 2006; 444:1032-7; PMID:17183313; http://dx.doi.org/10.1038/nature05355
52. Thurston G, Noguera-Troise I, Yancopoulos GD. The Delta paradox: DLL4 blockade leads to more tumour vessels but less tumour growth. Nat Rev Cancer 2007; 7:327-31; PMID:17457300; http://dx.doi.org/10.1038/nrc2130
53. Sainson RC, Harris AL. Anti-Dll4 therapy: can we block tumour growth by increasing angiogenesis? Trends Mol Med 2007; 13:389-95; PMID:17822956; http://dx.doi.org/10.1016/j.molmed.2007.07.002
54. Li JL, Sainson RC, Oon CE, Turley H, Leek R, Sheldon H, Bridges E, Shi W, Snell C, Bowden ET, et al. DLL4-Notch signaling mediates tumor resistance to anti-VEGF therapy in vivo. Cancer Res 2011; 71:6073-83; PMID:21803743; http://dx.doi.org/10.1158/0008-5472.CAN-11-1704
55. Borghese L, Dolezalova D, Opitz T, Haupt S, Leinhaas A, Steinfarz B, Koch P, Edenhofer F, Hampl A, Brüstle O. Inhibition of notch signaling in human embryonic stem cell-derived neural stem cells delays G1/S phase transition and accelerates neuronal differentiation in vitro and in vivo. Stem Cells 2010; 28:955-64; PMID:20235098; http://dx.doi.org/10.1002/stem.408
56. Hitoshi S, Alexson T, Tropepe V, Donoviel D, Elia AJ, Nye JS, Conlon RA, Mak TW, Bernstein A, van der Kooy D. Notch pathway molecules are essential for the maintenance, but not the generation, of mammalian neural stem cells. Genes Dev 2002; 16:846-58; PMID:11937492; http://dx.doi.org/10.1101/gad.975202
57. Imayoshi I, Sakamoto M, Yamaguchi M, Mori K, Kageyama R. Essential roles of Notch signaling in maintenance of neural stem cells in developing and adult brains. J Neurosci 2010; 30:3489-98; PMID:20203209; http://dx.doi.org/10.1523/JNEUROSCI.4987-09.2010
58. Zhen Y, Zhao S, Li Q, Li Y, Kawamoto K. Arsenic trioxide-mediated Notch pathway inhibition depletes the cancer stem-like cell population in gliomas. Cancer Lett 2010; 292:64-72; PMID:19962820; http://dx.doi.org/10.1016/j.canlet.2009.11.005
59. Monticone M, Biollo E, Fabiano A, Fabbi M, Daga A, Romeo F, Maffei M, Melotti A, Giaretti W, Corte G, et al. z-Leucinyl-leucinyl-norleucinal induces apoptosis of human glioblastoma tumor-initiating cells by proteasome inhibition and mitotic arrest response. Mol Cancer Res 2009; 7:1822-34; PMID:19861404; http://dx.doi.org/10.1158/1541-7786.MCR-09-0225
60. Shih AH, Holland EC. Notch signaling enhances nestin expression in gliomas. Neoplasia 2006; 8:1072-82; PMID:17217625; http://dx.doi.org/10.1593/neo.06526
61. Dirks PB. Brain tumor stem cells: bringing order to the chaos of brain cancer. J Clin Oncol 2008; 26:2916-24; PMID:18539973; http://dx.doi.org/10.1200/JCO.2008.17.6792
62. Bleau AM, Howard BM, Taylor LA, Gursel D, Greenfield JP, Lim Tung HY, Holland EC, Boockvar JA. New strategy for the analysis of phenotypic marker antigens in brain tumor-derived neurospheres in mice and humans. Neurosurg Focus 2008; 24:E28; PMID:18341405; http://dx.doi.org/10.3171/FOC/2008/24/3-4/E27
63. Yang ZJ, Wechsler-Reya RJ. Hit 'em where they live: targeting the cancer stem cell niche. Cancer Cell 2007; 11:3-5; PMID:17222787; http://dx.doi.org/10.1016/j.ccr.2006.12.007
64. Fan X, Mikolaenko I, Elhassan I, Ni X, Wang Y, Ball D, Brat DJ, Perry A, Eberhart CG. Notch1 and notch2 have opposite effects on embryonal brain tumor growth. Cancer Res 2004; 64:7787-93; PMID:15520184; http://dx.doi.org/10.1158/0008-5472.CAN-04-1446
65. Wang J, Wakeman TP, Lathia JD, Hjelmeland AB, Wang XF, White RR, Rich JN, Sullenger BA. Notch promotes radioresistance of glioma stem cells. Stem Cells 2010; 28:17-28; PMID:19921751
66. Binderup T, El-Ali HH, Ambrosini V, Skovgaard D, Jensen MM, Hesse B, Jorgensen JT, Kjaer A. Molecular Imaging with Small Animal PET/CT. Curr Med Imaging Rev 2011; 7:234-47; http://dx.doi.org/10.2174/157340511796411221